Analysis of the Influence of Pantographs in Railway Communications

Magali Mendes Correia, Luís M. Correia
Instituto Superior Técnico / INOV-INESC
University of Lisbon
Lisbon, Portugal
magali.correia@tecnico.ulisboa.pt
luis.m.correia@tecnico.ulisboa.pt

Fernando Santana
Thales
Lisbon, Portugal
Fernando.santana@thalesgroup.com

***Abstract*— In high-speed railways, there are several interference sources. The interference caused by the pantograph, an element that collects the current from the power supply and the catenary structure that transports the power, is one of them. Its importance is due to the effect that has on the railway communications and, consequently, the safety on the high-speed railway. The main objective of this thesis was to analyse the performance of antennas for four different railway communication systems when influenced by the pantograph and the catenary. The communication technologies considered were TETRA, with a working antenna operating at 380MHz, GSM-R at 900MHz, LTE-R at 2.6GHz, and BBRS at 5.9GHz. Two different approaches were taken to analyse the problem. The first one, regarding the antenna analysis, consisted of the development of a model based on the CST software, where one considered the antennas' parameters, as well as the pantograph/catenary structures. One identified four different scenarios regarding these structures: only rooftop (reference scenario), rooftop and catenary, rooftop and pantograph, and rooftop plus catenary and pantograph. The models for these scenarios were developed, and the results were analysed through radiation pattern, reflection coefficient, half-power beamwidth, and the first side lobe level. The second approach, regarding electromagnetic interference, consisted of determining the minimum Signal-to-Noise-Plus-Interference-Ratio mathematically. One used the CST model for the rooftop and catenary scenario to determine the interference power from the catenary, and then discovered the power correspondent to each of the four harmonics (380MHz, 900MHz, 2.6GHz, and 5.9GHz).**

Keywords – Railway Communication, Pantograph, TETRA, GSM-R, LTE-R, BBRS, Electromagnetic Interference.

I. INTRODUCTION

Mobile communications have undergone an impressive evolution in recent decades, showing any sign of slowing down. They became a fundamental part of the quotidian both on a personal and a professional level.

It all began with the 1st Generation (1G) emerging in the 1980s, which used analogue technology and allowed only voice communications. The 2nd Generation (2G) surges in the early 1990s, and it uses digital technology and will enable data communications, despite being designed only for voice. Global System for Mobile (GSM) was the first digital mobile communication system. It provides both voice and data services for a more substantial number of users, firstly through circuit-switched technology and then by packet-switching. In railway communications, GSM-R became the world standard. It is based on the commercial system GSM but has been specially designed to meet railways' requirements. The system has a 200kHz bandwidth, using Time Division Multiple Access (TDMA), where one TDMA frame corresponds to 4.615ms and is constituted by 8 time-slots with 156.25bits each (577us). The GSM-R system has a capacity of 22.8kbps for voice services and 9.6kbps for data transmission [1]. Today, this is still the standard for railway communications.

In response to the constant evolution of services and the growing need for higher data rates, surges the Long Term Evolution (LTE), in the late 2000s, as the 4th Generation (4G). It respects all 3GPP specifications presented in Releases 7, 8, and 9. The system achieves maximum downlink (DL) peak rates of 300 Mbps and uplink (UL) 75 Mbps. The future mobile radio system for railways is LTE-R, created to provide improved and more efficient transmission for High-Speed-Railway (HSR) communications, which is based on an IP based packet switched solution.It may operate in 70 different frequency bands, either for LTE Frequency Division Duplexing (FDD) or for LTE Time Division Duplexing. Presently, most LTE systems work at the bands above 1GHz, such as 1.8, 2.1, 2.3, and 2.6GHz. The available LTE carrier bandwidth goes from 1.4MHz, with 72 reserved subcarriers, to 20MHz, with 1200 subcarriers, depending on the number of sub-carriers needed with a 15kHz separation between them [2]. Despite this, LTE-R has not yet been standatised

TETRA, TErrestrial Trunked RAdio, was developed and standardized by the European Telecommunication Standards Institute (ETSI), it is an example of a Professional/Privat Mobile Radio (PMR) system, used mainly for professional situations by the government or official entities. It operates in the 400MHz and 800MHz bands, but for railway applications, usually the dedicated frequencies are in the 400MHz band. TETRA uses TDMA technology. For each 25 kHz carrier, exists four channels, which allows 4 data or voice calls. The maximum number of carriers for the BS is eight, adding up to 32 times

slots. The maximum transmitted data is to 28.8kbps, 7.2kbps for each channel [3].

BBRS is a railway communication system provided by Thales. It allows the transmission and reception of data between the infrastructures (i.e., stations) and the trains. Security systems such as CCTV and the systems for management of trains are some examples that need BBRS to function. This system uses channels with a bandwidth of 20MHz or 40MHz. Since the wireless network uses an OFDM modulation, it more than doubles the data rate. With a 20 MHz channel, OFDM slices it in 52 subcarriers, 48 of which used for carrying data. When the channel bandwidth is 40 MHz, the number of subcarriers carrying data increases to 144. This allows a data rate delivery of 65Mbps for a 20MHz channel and a total of 135 Mbps for a 40MHz channel [4].

The goal of this thesis is to analyse how the pantograph influences the performance of the antennas, affecting, therefore, the railways communication and endangering the quality of service provided to the passengers and railway operations. A model is going to developed and implemented using simulation software, the Computer Simulation Technology (CST) Microwave Studio.

The paper structure is as follows: Section I – Introduction; Section II – State of the art; Section III – Models and Simulator Description; Section IV – Results' Analysis; Section V – Conclusion.

II. State of the Art

In this section, an overview of research related to the subject of the thesis is presented in this subsection, where one shows the work that was developed in analysis the influence of pantograph and catenary in railway communications

[5] presents a thorough analysis of the electromagnetic interference generated by trains. This paper focus on the modelling of EMI received by antennas placed on the train roof. According to this study, the switch-on transients when the pantograph touched the contact wire and the switch-off when it detached, closing and opening the circuit respectively, creates interference and generates an electric arc. The researchers tried to reproduce the four different stages of the pantograph, by switching on and off the High-Speed Circuit Breaker (HSCB) and connecting ad disconnecting the pantograph from the catenary. The tool Computer Simulation Technology (CST) was used to modulate the most representative train components.

In [6], the researchers pointed out the importance of understanding the EMI in electric railways due to the interaction between the pantograph and the overhead contact line. In [7], the same authors as before present the results of a measurement campaign aimed at investigating EMI phenomena

In [8], the author's objective is to understand the transient disturbances produced by the pantograph in the train's roof and analyse the EMI disturbance received by GSM-R antennas. The measurements were made on the OARIS high-speed train provided by a Spanish rolling stock company. The measurements made for the EM disturbances coming from the catenary-pantograph are the main focus, and this analysis was supported by the CST tool.

An assess on the contribution of the arc channel to the total emission is presented in [9], along with experimental evidence that this contribution is negligible compared to that of the rest of the circuit. The main objective was to determine whether electromagnetic emission can be associated with only the arc or with the all-electric and geometric characteristics of the circuit in which the discharge takes place

[10] presents an overall explanation of the consequences of pantograph arcing in the AC traction system. It approaches the distortion of the sinusoidal waveform cause by the pantograph arcing, as well as the harmonics and inter-harmonics, conducted and radiated electromagnetic emission, which can cause interference in several radio-based communication systems.

In [11], the authors assess the low-frequency electric and magnetic field of AC 25kV/50Hz power supply systems. Measurements of the electric field strength were performed and compared with the calculation's results, which, when compared, shown a good agreement

André Ribeiro's thesis [12], provides analyse of the performance of antennas on trains and understand the impact of the different available positions to install the antennas depending on the surrounding environment, to optimise and improve services for railway operations and passengers experience. Using CST tool, it was possible to import similar 3D models of trains and train antennas of different mobile communications systems (GSM-R, LTE-R and BBRS) and to perform a complete analysis of the antenna's parameters.

III. Models and Simulator Description

A. Model Description

After analysing the problem, it was defined that it could be divided into two main issues:

- The presence of two metallic structures, pantograph and catenary, in the surroundings of the antenna.
- The harmonics from the catenary due to its electric field that have the same frequency as operating frequency of the antenna.

An example of the typical scenario can be observed in Figure 1.

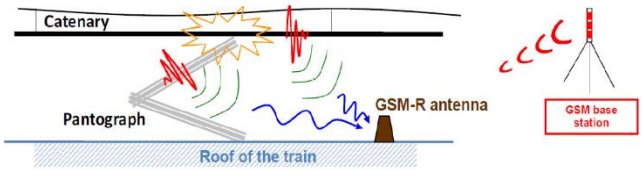

Figure 1. Pantograph and Catenary (from [13])

Figure 2. presents the model overview, with the input parameters, the simulations performed, and the output parameters.

This said that the model consists on the design of an antenna model using Antenna Magus, that will be used along with a train/pantograph/catenary model in CST Microwave Studio. After the simulations in CST, the results include a 2D and 3D

Radiation Pattern, Half Power Bandwidth (HPBW), the reflection coefficient, the first side lobe level and the electrical field. This last result will be used yet in MATLAB to obtain the power from harmonics resulting from the catenary and the Signal-to-Noise-plus-Interference-ratio.

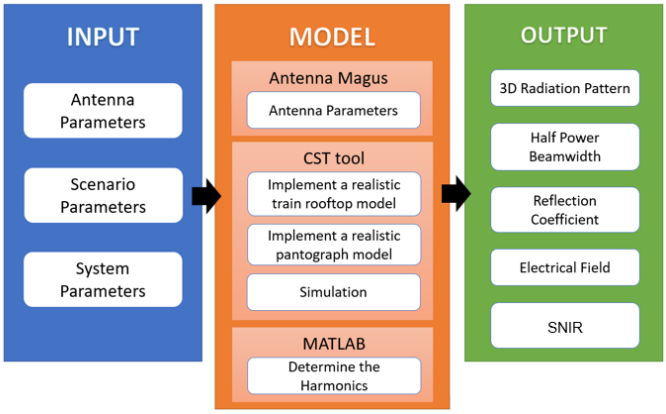

Figure 2. Model overview

Regarding the first part of this work, the antenna analysis, the assessment on how the performance of the antenna is affected when in the presence of two metallic structures, pantograph and catenary, is done. In this case study, the antenna is present in the train's rooftop, which is considered to plane. The transmitted and received waves of a radiating element that are directed to the ground suffer a reflection that has different behaviours depending on the geometry of the problem, the ground characteristics, frequency, or antennas' specifications. To simplify the problem, one must consider the roof of the train, a flat ground, infinite and a Perfect Electric Conductor (PEC).

For the second part of this work, the EMI analysis, the signal that one considers passing through the catenary and pantograph corresponds to the sum of the original signal, a 25kV AC with $f_0 =$ 50Hz, and the harmonics of certain order N_harm, which frequency is 380MHz, 900MHz, 2600MHz, and 5900MHz. It can be expressed as

$$x'(t)_{[\mathrm{V}]} = \sum_{n=0}^{N\_harm} \frac{25000}{N\_harm} \cdot \sin(2\pi \cdot N\_harm \cdot f_{0_{[Hz]}} \cdot t) \quad (1)$$

A periodic time-domain signal can be represented as a sum of sinusoidal signals. The Fourier Series, Trigonometric and Exponential, of a periodic function x(t), can be expressed as

$$x'(t) = \sum_{n=1}^{\infty} c_n e^{jn\omega_0 t} \quad (2)$$

The exponential Fourier coefficient, c_n , stablishes the relation between the electric field from the fundamental frequency, the one obtained using CST, and the following harmonics. They can be obtained using the following expression

$$c_n = \frac{1}{T_0} \int_0^{T_0} x'(t) e^{-jn\omega_0 t}\, dt \quad (3)$$

To calculate the theoretical value of the electric field, one considers this scenario equivalent to a cylindrical conductor parallel to a ground conductor, as presented in Figure 3.

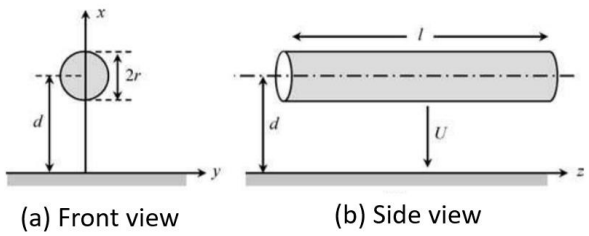

Figure 3. Cylindrical conductor above ground

The expressions for the capacitance and the electric field were used

$$C_{[\mathrm{F}]} = 2\pi \cdot \epsilon_{0_{[\mathrm{F/m}]}} \cdot \frac{1}{log_{10}\left(\frac{d_{[\mathrm{m}]}}{r_{[\mathrm{m}]}} + \sqrt{(d_{[\mathrm{m}]}/r_{[\mathrm{m}]})^2 - 1}\right)} \quad (4)$$

$$E_{[V/m]} = \frac{C_{[\mathrm{F}]} \cdot U_{[V]} \cdot d_{[\mathrm{m}]}}{\pi \cdot \epsilon_{0_{[\mathrm{F/m}]}} \cdot l_{[\mathrm{m}]} \cdot ({x_{[\mathrm{m}]}}^2 - {d_{[\mathrm{m}]}}^2)} \quad (5)$$

To determine the power of each interfering harmonic, the following expression was used

$$P_{harm_{[dBm]}} = -77{,}21 + E_{[dBuV/m]} + G_{[dBi]} - 20\log(f_{[MHz]}) \quad (6)$$

The theoretical gain for λ/4 monopole over an infinite an infinite ground plane is 5.19dB. To determine the minimum SNIR, the sensitivity and the interfering power were determined. The following expressions were used

$$SNIR_{\min[dB]} = \frac{P_{min\ [dBm]}}{N_{[dBm]} + I_{[dBm]}} \quad (7)$$

$$N_{[dBm]} = -174 + 10\, log_{10}(\Delta f_{[Hz]}) + F_{[dB]} \quad (8)$$

B. Train/Pantograph/Catenary Model

In terms of the scenario that is analysed, the train, the pantograph, and the catenary are the main structures that one is going to focus on. The CST model needed to represent the scenarios presented in Figure 4.

Figure 4. Pantograph and Catenary – Azambuja's station

To do so, a model from a CAD database was obtained. However, the simulation time regarding this model, that presented a complete carriage, and the pantograph was taking more than 10 hours to simulate for lower frequencies. So, to diminish the simulation time, one focuses on the rooftop pantograph and catenary. The pantograph structure had to be

completely redone to have a more simplify model, since, due to details, simulation time for higher frequencies were higher than three days. The final model is presented in Figure 5.

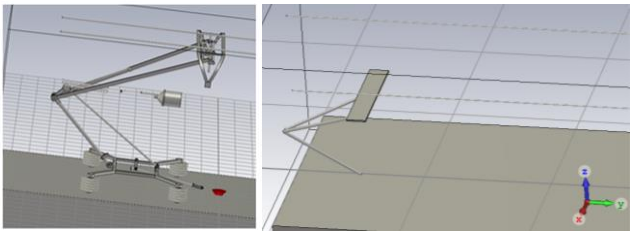

(a) Before (b) After

Figure 5. Pantograph-Catenary CST model

C. Model Assessment

Firstly, an evaluation of the isolated antenna performance is done. To understand the behaviour of the antennas' parameters, a $\lambda/4$ resonant monopole is chosen because of the rooftop morphology, and also because a monopole working above an infinite ground plane is the equivalent to a $\lambda/2$ resonant dipole. This approach is suitable because monopoles are usually installed inside an aerodynamic structure. The antennas considered were a 380 MHz working frequency for TETRA, 900 MHz for GSM-R, 2.6 GHz for LTE-R, and 5.9 GHz for BBRS.

Some specific antenna parameters such as the centre working frequency, the minimum and maximum frequencies, the directivity or the realised gain, and the port impedance characteristics, such as S_{11} and the characteristic impedance Z_0 were set. In this case, de impedance of the $\lambda/4$ monopole is only resistive (36.5 Ω), with zero reactive impedance.

These four antennas were imported to CST, where the simulation was run. The main objective was to understand if the obtained performance results are similar to the theoretical ones. All the simulations were based on the Time Domain Solver and the global properties set at "Hexahedral". Regarding simulation time, the most critical case is the 5.9 GHz, due to the smallest wavelength, creating 251,464 mesh cells. The simulation took about 21 hours, which is acceptable.

Regarding the antenna analysis, to understand if the model selected to evaluate the behaviour of the antenna in the presence of the catenary and pantograph is correct, one had to look to the simulation results. Looking to the reference scenario, where the only structure besides the antenna is the train rooftop, one can observe that the gain obtained in the simulation, 5.273 dBi, is similar to the theoretical one, 5.19 dBi, as presented in Figure 6.This means that the presence of the train rooftop in the antenna is not significant, so all the results obtained with the catenary and the pantograph will be mainly affected by these.

For the EMI analysis, one took the theoretical approach firstly. Using the theoretical expression on MATLAB, one determined the exponential coefficients for the harmonic correspondent to each technology and the value of the electric field for the distance of reference, 1.4m. The result obtained, E = 6338V/m, corresponds to the electric field prevenient from the fundamental frequency, 50 Hz. Having both information one can determine the value of the electric field from each harmonic and then its power. In the simulation approach, one uses the CST to simulate this same scenario and determine the maximum value of the electric field

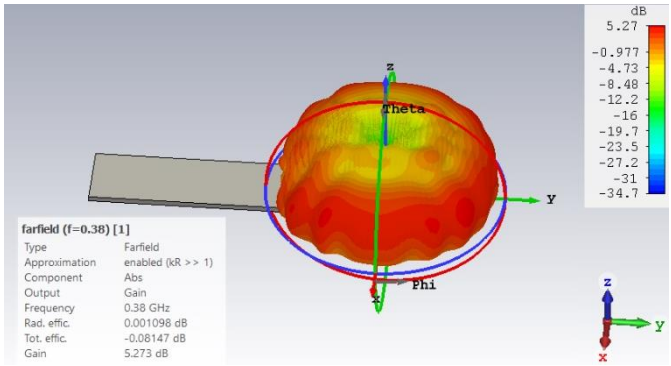

Figure 6. 3D farfield view at 380 MHz

For the EMI analysis, one took the theoretical approach firstly. Using the theoretical expression on MATLAB, one determined the exponential coefficients for the harmonic correspondent to each technology and the value of the electric field for the distance of reference, 1.4m. The result obtained, E = 6338V/m, corresponds to the electric field prevenient from the fundamental frequency, 50 Hz. Having both information one can determine the value of the electric field from each harmonic and then its power. In the simulation approach, one uses the CST to simulate this same scenario and determine the maximum value of the electric field

The value obtained in the simulation was E_{max}=4481.7 V/m, which divided by $\sqrt{2}$ provides the average time value of E = 3446 V/m. The difference in the results may be due to CST assuming that the potential between the catenary and the train rooftop is continuously 25kV, when theoretically is periodic. Also, the train rooftop is not an infinite structure as it is theoretically assumed, so this may also be affecting the results. Figure 7. presents the power od each interfering harmonic for a distance between the catenary and rooftop of 1.4m. As expected, since the signal amplitude decreases as the order of the harmonic increases, the resulting interfering power also decreases.

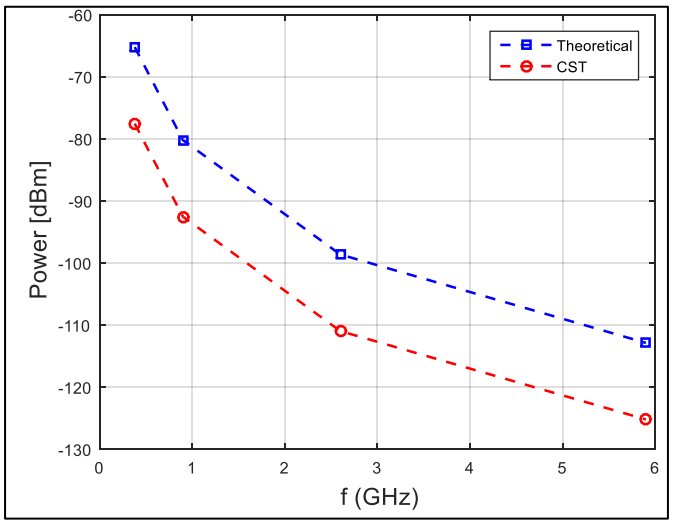

Figure 7. Harmonic's Interfering power

IV. Results' Analysis

In this section, a description of the reference scenario for both the antenna analysis and the EMI study is provided.

A. Scenario Description

Generally, the train rooftop is a curved ground with specific dimensions. However, since the goal of this work is to analyse the antenna performance in the presence of the pantograph and catenary, one has considered that the train rooftop is a plane rectangular metallic structure. The dimensions for the scenario are presented in Figure 8.

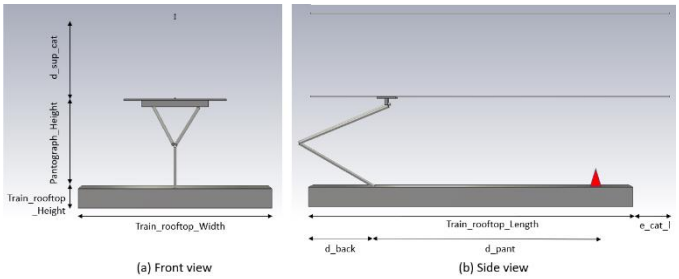

Figure 8. Rooftop/Pantograph/Catenary CST model

Each dimension is defined as follows:

- d_sup_cat: Distance between catenary and the support line.
- d_pant: Distance between the front of the carriage and the pantograph.
- d_back: Distance between the back of the carriage and the pantograph.
- e_cat_l: Extra catenary length, about 5λ.
- Pantograph_Height: Height of the pantograph.
- Train_rooftop_Height: Height of the train rooftop, 30cm.
- Train_rooftop_Length: Length of the train rooftop, variable.
- Train_rooftop_Width: Width of the train rooftop, 3m.

For the antenna analysis part, the values for each of these dimensions, according to each system are presented in Table 1. (based on [14]).

Table 1. Model dimensions for Antenna analysis

f [MHz]	380	900	2600	5900
d_sup_cat [m]	1.3			
d_back [m]	1			0
e_cat_l [m]	4	1.7	0.6	0.3
Pantograph_Height [m]	1.4			
Train_rooftop_Height [cm]	30			
Train_rooftop_Length [m]	18	9	5	4
Train_rooftop_Width [m]	3			

One has also chosen three distances between the antenna and the position of the pantograph (d_pant) for each technology: one outside the 20λ limit, and the other two inside. This way is possible to assess what is the 5ehavior of the antenna when the pantograph is both outside and inside of the antenna's influence radius. The selected distances are presented in Table 2.

Concerning the analysis of the signal received at the antenna, one can distinguish two placements for the antennas: the on-track radios and the on-board radios. The BSs are placed parallel to the railway, equally distanced, and the MSs are usually in each extremity of the carriage. Although this information is important when approaching the problem, the main focus when 5ehavior5 the antenna resides on the two perspectives between an antenna and the BSs: the vertical perspective (elevation plane) and horizontal plane (azimuth plane), as presented in Figure 9.

Table 2. Distances between antenna and pantograph

f [MHz]	20λ [m]	d_pant [m]		
380	15.8	16	10	5
900	6.7	7	4	1
2600	2.3	3	2	1
5900	1.0	1.25	1	0.5

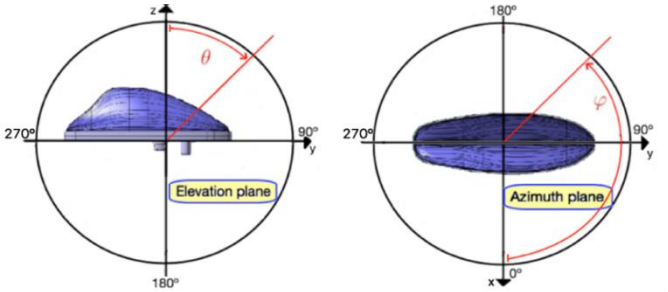

Figure 9. Antenna perspectives

The elevation plane provides information regarding the elevation angle θ, which is measured between the BS and the antenna. When θ = 0°, this means that the antenna is passing right under the BS, and when θ = 90°, both antennas are at the same height, and this may be due to the terrain morphology. The azimuth plane gives the direction and positioning of the antenna relative to the BS from the angle φ. For example, if φ = 0° V φ = ±180°, then the BS would be at the right or left of the train, and when φ = 90° V φ = 270°, the BS respectively in the same direction of the movement of the train or the opposite direction. This information is relevant to decide which angles are important to assess the antennas' 5ehavior, as one presents in the following section. In this study, one is going to assess two sets of angles.

For the first part of this study, the four scenarios that one considered are the following: only rooftop (R), rooftop with catenary (R+C), rooftop with a pantograph (R+P), and rooftop with catenary and pantograph (R+C+P), all of them presented in Figure 10. These last three will be compared with the reference scenario, R, where there is only the antenna placed on the rooftop. Regarding the problem formulation, one has analysed three different perspectives in the azimuth plane: φ = 0° (lateral view), φ = 90° (no pantograph obstruction), and φ = 270° (possible pantograph obstruction).

For the second part of this study, one considered only the R+C+P scenario. Regarding the problem formulation, one has analysed eight different perspectives in the azimuth plane: φ = 45°, φ = 60°, φ = 75°, φ = 90°, φ = 270°, φ = 285°, φ = 300° and φ = 315°; and different elevation angles in the interval [60°;90°], with a step size of 5°. This set of angles was chosen because the

most important scenario is when the trains are between BSs when the performance of the antenna can be more critical due to the distance to the BS that is serving, as shown in Figure 11.

Figure 10. CST models

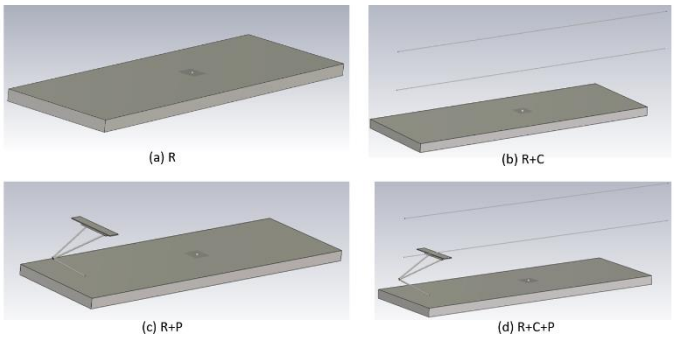

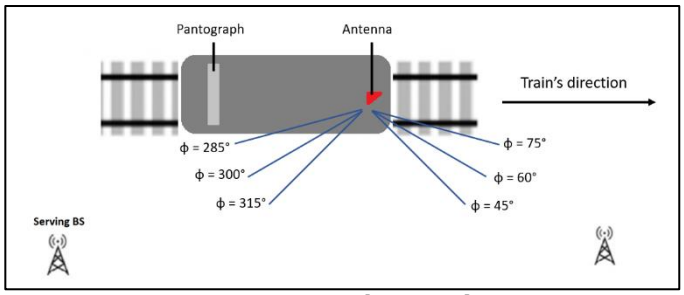

Figure 11. Train horizontal view

For the second part of this study, the EMI analysis, the values for the parameters presented in Figure 8. are presented in Table 3.

Table 3. Model dimensions for EMI analysis

d_sup_cat [m]	1.3			
e_cat_l [m]	0			
Pantograph_Height [m]	1.2	1.4	1.6	2.8
Train_rooftop_Height [cm]	30			
Train_rooftop_Length [m]	10			
Train_rooftop_Width [m]	3			

Table 4. presents the values for the parameters presented in Chapter 3, such as the noise figure, the carrier bandwidth, and the sensitivity, for each system, provided by Thales.

Table 4. EMI input parameters

f [MHz]	**380**	**900**	**2600**	**5900**
N [dB]	8	8	7	5
Δf [kHz]	25	200	15	384
$P_{min\ [dBm]}$	-103	-104	-94	6Mbps: -90 54Mbps: -73

B. *Antenna analysis*

In this section, an analysis is performed to determine the effect that two obstacles, the pantograph, and the catenary, have on the antennas' performance. The height of both structures is variable. However, one decided that 1.4m between them would be a reasonable height. Two studies were performed in this section: one comparing four different scenarios and other varying the distance between the catenary and the pantograph.

1) *TETRA*

One started the simulations in CST using the TETRA antenna, with an operating frequency of 380 MHz. The simulations were ran using the four scenarios presented before and the three distances d_pant: 16m, 10m, and 5m. For the first part, one has chosen to analyse the results for d_pant=10m, within the 20λ boundary, which are presented in Figure 12.

When φ=0° (side view), the antenna's performance is very similar in the four scenarios. One observes a slight variation of 1.26dB in the gain, along with an α_{3dB} between 39.5° and 49°. The direction of maximum gain decreases 8-11 degrees in the scenarios with a pantograph and/or catenary relatively to the reference. This may not be relevant since, for the most part, the BSs are at the front or the back of the train. For φ=90° (front view), one observes a significant improvement in the antenna performance when in the presence of pantograph and/or catenary, increasing about 5dB. However, this growth is accompanied by the increasing of the direction angle, which means that these structures lead to the reflection of the electromagnetic waves in this direction, increasing the gain magnitude. The directions of maximum gain, between 83-88 degrees, means that the antenna is directed in a straight line in this direction, which can be unfavourable, especially on terrain with irregular morphology.

When φ=270° (back view), one observes that only on the R+C+P scenario, the performance of the antenna is significantly above the reference, increasing 5.14dB, along with a low α_{3dB}. The low dispersion of the electromagnetic waves increases the gain magnitude. Thus, in the presence of both structures the directivity of the antenna increases, affecting the omnidirectional behaviour of the antenna. Also, in the R+P

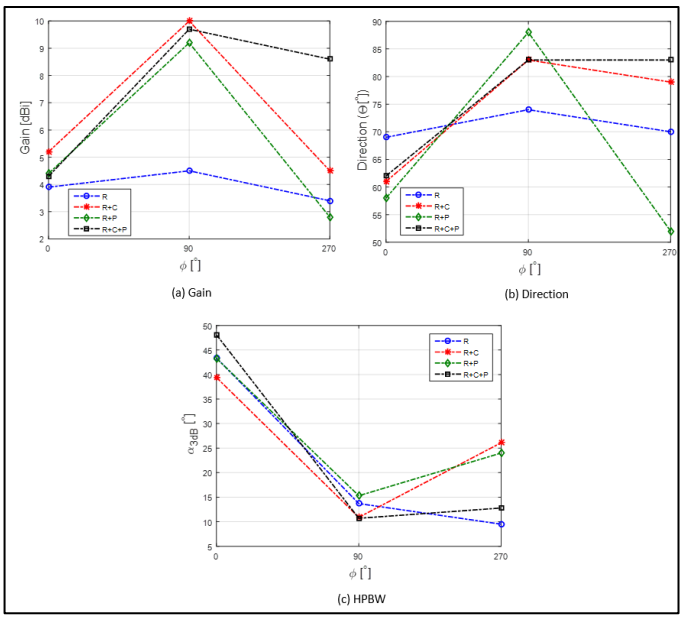

Figure 12. Comparison between scenarios at 380MHz

scenario, the direction angle is expressively lower than the reference, along with a maximum gain slightly below the

reference. This means that the pantograph reflects the EM waves propagation in all directions except for this one, in particular, in the opposite direction, which may lead to communication problems with the BS behind the train.

To understand the behaviour of the antenna when varying the pantograph antenna distance in the R+C+P scenario, a set of angles where selected. Figure 13. and Figure 14. present the results obtained for the three distances in eight azimuth angles, four correspond to the front of the train, and the other four to the back of the train, respectively, as well as the standard variation. One observes that at distances d_pant equal to 5m and 10m, within the influence range of 20λ, the behaviour of the antenna is very close to the reference scenario for the φ=45° and φ=60°, decreasing less than 1dB, and increasing from 1.5dB to 2.5dB for φ=75° and φ=90°, so the pantograph improves the antenna's performance. For d_pant equals to 5m and φ=75° and φ=90° perspectives, the standard deviation is between 4dB and 5dB, so the antenna's directivity increases when the antenna is in the presence of the catenary and pantograph. When moving away from the antenna, the standard deviation decreases, so the antenna is no longer as directive as before, which leads to a decrease in the generalized gain. For d_pant equal to 16m, the generalised gain decreases significantly, verifying that the presence of the pantograph is no longer felt. However, the catenary is still above the antenna, which leads to a significant decrease in φ=90°In the back part of the train, the equivalent happens for symmetric angles, being the generalized gain for φ=285° slightly more significant than in the front part of the train, but then the tendency is to get closer to the reference as the antenna moves away from the pantograph. However, when φ=285°, the standard deviation of the gain increases, which means that the reflexion from the catenary is being felt and leading to a more directive antenna behaviour.

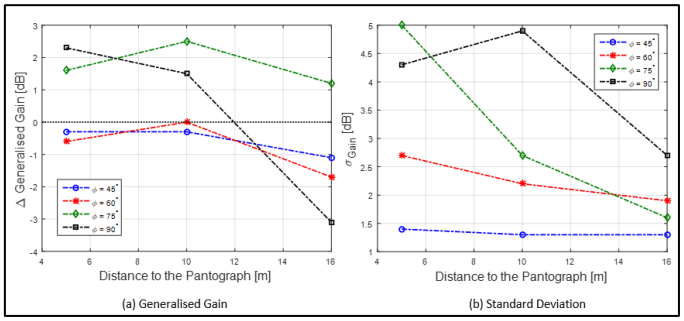

Figure 13. Comparison at the front part of the train

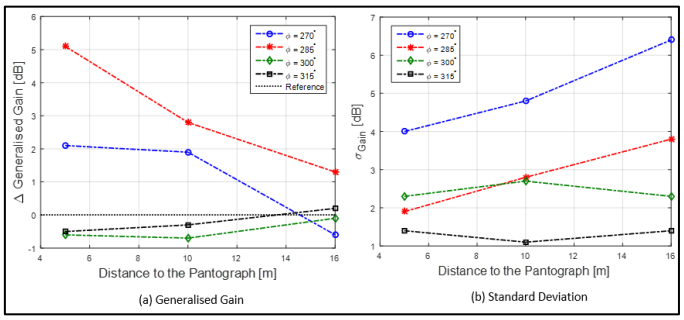

Figure 1. Comparison at the back part of the train

2) GSM-R

For GSM-R, one has used an antenna operating at 900MHz. The simulations for the four scenarios and three distances were run in CST. Figure 15. presents the comparison of the antenna performance for the four scenarios when the antenna is at 4m from the pantograph base. Notice that at this distance, the antenna is nearly in the middle of the train rooftop and inside of the 20λ boundary. One observes that once again, in the lateral view (φ=0°), the maximum gain increases meaningfully comparatively to the reference, intensifying 7-9dB. This is accompanied by huge growth in the direction angle, with the antenna pointing much lower, between 65-70 degrees, so the presence of the catenary and/or catenary reflects the EM waves in this direction. However, α_{3dB} decreases 1.1° and 2.5° for R+C and R+C+P scenarios, respectively, and it remains practically constant in the R+P scenario, so the catenary is responsible for decreasing the EM waves dispersion, leading to a more directive antenna. Once again, this may not be an issue for this perspective since the BS is right beside the carriage and its power is very high.

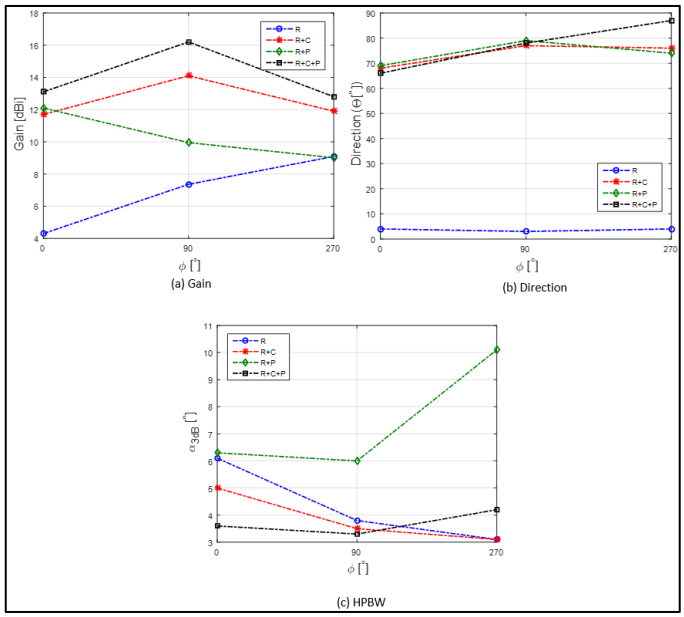

Figure 15. Comparison between scenarios at 900MHz

In the front view (φ=90°), one observed that the presence of the catenary continuous to increase the maximum gain in this perspective, along with a high direction and an α_{3dB} below reference, so the antenna still has a directive behaviour. However, in the R+P scenario, one observes a clear decrease of the gain with an α_{3dB} 2.9 degrees above the reference, so the dispersion of EM waves increases, which could lead to interference problems regarding other signals. For φ=270°, the back view, one observed that, in terms of gain, only in the R+P scenario, it equals the reference, along with an α_{3dB} of 10.1 degrees, so the reflection on the back of the train is very dispersive due to the pantograph.

Regarding the generalized gain and the standard variation, in the front part of the train, one observed that for φ=45° and φ=60°, the generalized gain is very close to the reference for all distances from the pantograph, varying about 1dB, so the catenary and the pantograph do not have a significant effect on

the antenna behaviour for these perspectives. For φ=75° and φ=90° in the two distances within 20λ boundary, the generalised gain is about 4dB to 6dB above the reference, so the antenna has a very directive behaviour. When d_pant equals to 7m, the generalised gain for φ=75° decreases significantly, and remains almost constant for φ=90°, so the EM waves are mostly reflected in this direction. Regarding the standard deviation, inside the 20λ limit, it is clear that, for φ=45° and φ=90°, the lobe is very irregular. When d_pant equals to 7m, outside the 20λ boundary, σ_{Gain} tends to zero, so the effect of the pantograph is much more significant than the catenary. In the back part of the train, one observed that when the antenna is moving away from the pantograph, σ_{Gain} increases for φ=270° and φ=285°, so the influence of the catenary is much more significant when the pantograph is not close to the antenna. In terms of σ_{Gain}, one observed that for φ=270°, when d_pant is to closed to the pantograph, it is about 3dB, but when it moves away but and is still inside the 20λ boundary, it increases to almost 8dB, so the lobe is much more irregular due to the reflections in the pantograph. When d_pant equal to 7m, the influence is no longer felt, so σ_{Gain} decreases again.

3) LTE-R

For LTE-R technology, the antenna used is operating at 2.6GHz. The results for d_pant=2m, in the three perspectives, are presented in Figure 16. For φ=0°, one observed that in the R+P scenario, the gain increases about 2dB relatively to the reference, along with a 5° increase in the direction, and a decrease of 5.8° in the α_{3dB}, so the antenna has a more directive behaviour comparatively to the reference. The pantograph reflects the EM waves in a way that there is less dispersion, which increases the gain. For the R+C and R+C+P, the existence of the catenary leads to an even more significant increase in the gain and on the direction, and a decrease of the α_{3dB}, so the antenna is even more directive with the presence of the catenary. One observed that for both φ=90° and φ=270°, the maximum gain for all the three scenarios with the structures is below the reference, so the antenna is too close to the pantograph, and the EM waves are being reflected the sides (φ=0° and φ=180°). This could be a very significant issue, since, as mentioned before, the BSs are mostly at the front or the back of the train, so the pantograph and the catenary are considerably damaging the performance of the antenna in these views. One also observed that for the front and the back view, the direction is more or less equal, except for the R+C scenario, but this is because the antenna is very close to the back end of the carriage (3m) comparatively with the 7m in the opposite direction. Regarding the α_{3dB}, one observed that, for φ=0°, its value is much lower in scenarios with a pantograph and/or catenary, which supports the conclusion of the gain increasing on the sides, making the antenna more directive in that perspective.

Regarding the variation of the generalised gain and the standard variation, one observed that, in the perspectives on the front part of the train, the generalised gain is, for the most part, below the reference. In particular, when the antenna is outside of the boundary of influence of the pantograph, in φ=60°, φ=75°, and φ=90° perspectives, the generalised gain decreases significantly. This means that the catenary is harmful to the antenna performance, especially in this range of angles, and that the pantograph reduces its impact. As on has mentioned before, the transitioning from one BS to another is the most critical scenario due to the distance between the antenna and the BSs themselves, so when having a low gain in these perspectives, some railway operations may be vulnerable. One also observed that for φ=75° and d_pant equals to 3m, σ_{Gain} increases meaningfully, so the antenna is very directive in this direction.

In the back part of the train, one observed that when the antenna is 1m from the pantograph, the generalised gain for φ=270° and φ=285° is below the reference, so the antenna is so close to the pantograph that the EM waves are mostly reflected in the opposite direction (φ=90°). This means that when the train is stepping away from the BS, the railway operation may suffer a severe quality decrease. As the antenna moves away from the pantograph, one noticed that for φ=270°, the generalized gain increases, being significantly above the reference when outside the 20λ limit, so the reflection of EM waves is significant in this direction. The proximity to the pantograph is substantial here, because it either damages the antenna performance, resulting in communication issues, or it improves it, which leads to possible interference issues. Regarding σ_{Gain}, one observed that for a very close distance, its value is high for φ=270°, so the antenna is directive in this direction, and for a d_pant=3m, its high for φ=300°.

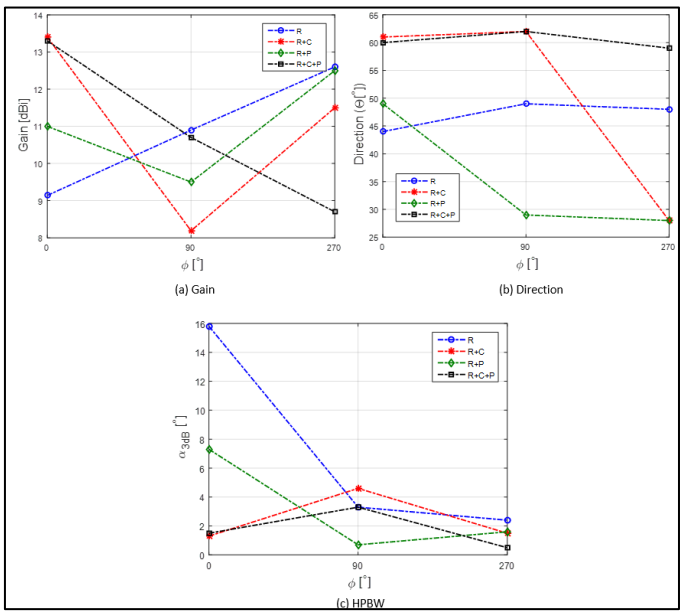

Figure 16. Comparison between scenarios at 2.6GHz

4) BBRS

One finally simulated CST using a BBRS antenna operating at 5.9GHz. Figure 17. presents the results obtained for a distance between the antenna, and the pantograph equals to 1m. For φ=0°, one observed an improvement in the antenna's performance. The maximum gain is approximately 2dB above the reference in the scenarios where the catenary is present, and 4.25dB above when there is only the pantograph. However, in the R+C+P scenario, the antenna is pointing in the 70° direction, while in the is pointing upwards. This, along with an α_{3dB} below the reference, means that the antenna has a more directive behaviour, losing the omnidirectional performance. As

explained before, this may not be a significant issue since in this case, the train is very close to the BS, so there would be performance problems. For φ=90°, the gain decreases, being slightly above the reference for R+P and R+C+P scenarios, whereas for R+C is 0.75dB below. This means that the antenna is so close to the pantograph, virtually underneath it, so there is not as much reflection of the EM waves in that perspective. In terms of the direction of maximum, the presence of the pantograph prevails that of the catenary, being 8°, which means that it is pointing up. This is a real issue since this perspective is critical when the train is between two BSs, so when the direction of maximum is up, the antenna is not directed to the BSs on the terrain, especially with this technology where the BSs are about 1km apart. The most common interval for the elevation angle would be from 60° to 90°, so this would result in severe link problems. For φ=270°, one observed that the performance of the antenna improves comparatively to the reference in all the scenarios, particularly the R+C+P scenario, where the gain magnitude increases 2.66dB. Also, the direction of the maximum is very close to the reference, from 13 to 30 degrees, along with a low α_{3dB}, so the antenna is very directive, and has its maximum pointing up. However, this case is not very realistic because the scenario that was used to run the simulation has the pantograph on the edge of the carriage, so the reflections of the EM waves in the rooftop are not considered. Also, the proximity of the antenna is not realistic.

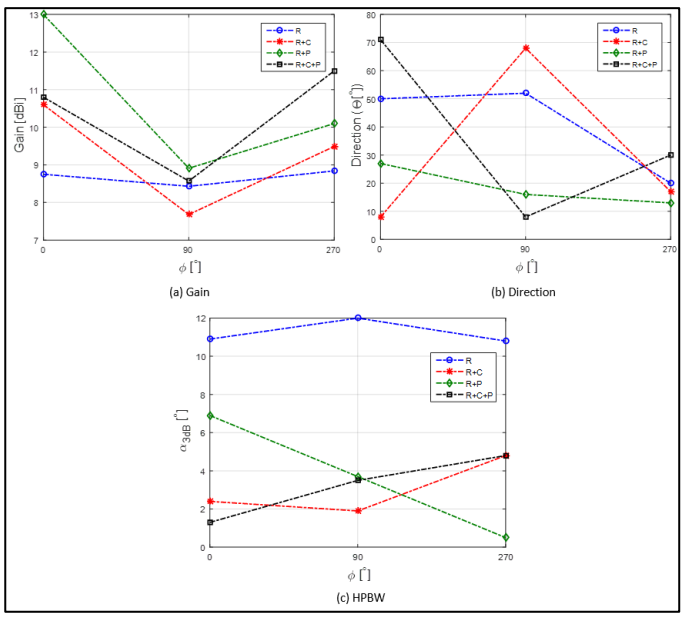

Figure 17. Comparison between scenarios at 5.9GHz

Regarding the variation of the generalised gain and its standard variation, one observed that the results for d_pant=0.5m and d_pant=1.25m are similar, so the behaviour of the antenna is the same when it is very close to the pantograph and outside of the 20λ boundary. This supports the fact that the antenna no longer feels a certain distance, the presence of the pantograph. For the front part of the train, when φ=45° and φ=60°, the generalised gain is about 2.5dB above the reference, but when φ=75° and φ=90°, it is between 5-6dB below, so the performance of the antenna is significantly damaged in the presence of the catenary and the pantograph, since this angles are significant when the trains are between BSs. As expected, one observed that for d_pant equals to 1m, the value of the generalized gain tends to the reference, since the antenna is almost at the limit of 20λ, and the reflected EM waves almost do not affect the antenna behavior.

In the back part of the carriage, where the pantograph is placed, for d_pant=0.5m and d_pant=1.25m, one observed that for all the azimuth angles, apart from φ=315°, the generalised gain is at or below the reference, along with a high σ_{Gain}. This means that the antenna is very directive and that is affected by the catenary. For d_pant equals to 1m, one observed an improvement in the generalised gain for φ=270° and φ=285°, so the pantograph is reflecting EM waves in these directions. Once again, this could lead to severe communications problems due to the reason presented before, but the probability of this scenario being deployed is very slim.

C. EMI analysis

The interference prevenient of the catenary is considered to be a noise since no information is being transmitted. The results obtained for Signal-to-Noise-plus-Interference-ratio are presented in Figure 18. One observed that when the catenary is closer to the train rooftop, the SNIR increases. This is expected since the electric field has a larger magnitude when closer to the catenary, which means that N_{cat} is highthe est. One also observed that the values of the SNIR is significantly higher than the sensitivity for each system, so the noise from the harmonics is high. This is expected since the signal in the catenary is in the order of kV, so the resulting electric field is also high. Only the BBRS system has a value close to the sensitivity (-73dBm) The values for the intermediate steps and the values for these parameters are available in Annex C. This means that the catenary presents a significant factor in railway communications which may lead to low quality of service or even failures is railway operations. One also must consider that these values are valid for the assumptions made in Chapter 3, where the amplitude of the harmonics decreases with a 1/n factor, which may not correspond to reality.

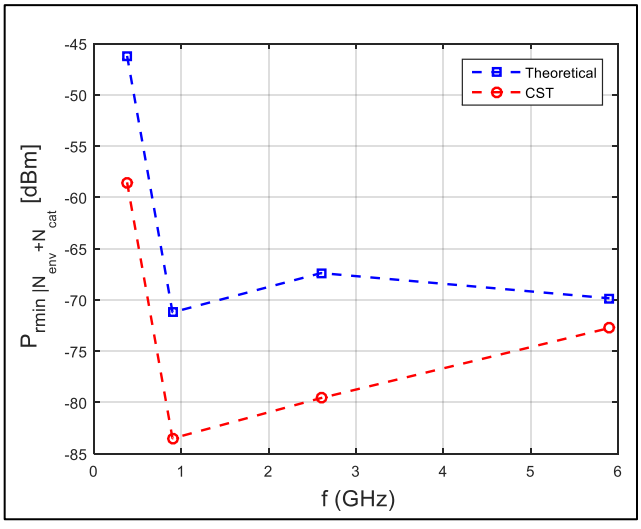

Figure 18. SNIR

One also analysed the difference in the minimum SNIR for two sensitivity values in BBRS, according to the correspondent

data rate. The results are presented in Table 5. One observed that for higher data rates, meaning lower sensitivity, the minimum SNIR is also lower. For a data rate of 54 Mbps, the SNIR is rounding the -86dBm to -90dBm, whereas for 6Mbps is between -69dBm and -73dBm. For a distance between the train rooftop and the catenary of 1.6m or 2.8m, the SNIR is equal to the sensitivity, so the noise from the catenary is not high enough in this case.

Table 5. SNIR for BBRS system

Data rate [Mbps]	$P_{min\ [dBm]}$		**d_sup_cat [m]**			
			2.8	**1.6**	**1.4**	**1.2**
6	-90	Theoretical	-89	-87	-87	-86
		CST	-90	-90	-89	-89
54	-73	Theoretical	-72	-70	-70	-69
		CST	-73	-73	-72	-72

V. CONCLUSIONS

The main goal of this thesis was to assess the influence of the pantograph and the catenary in the performance of the antennas for railway communications systems, as well as the impact of the harmonics prevenient from the catenary. The achieve these objectives, a model that represented this scenario was developed and implemented using CST for EM simulations, where several simulations where ran. Also, the MATLAB tool was used for all the numerical analysis. The results obtained from these simulations allow performing a thorough analysis of the effect of catenary and pantograph.

In the antenna analysis, one observed that in TETRA and GSM-R the presence of the catenary and the pantograph has an impact on the antennas' omnidirectional behavior. In LTE-R and BBRS the same is observed but it cannot be considered a realistic result since the proximity of the antenna to the pantograph is not something that one can observed in railway system.

Regarding the EMI, one observed that as the catenary is closer to the catenary, the power prevenient from the catenary is higher, which results in a higher minimum SNIR. The values obtained are significantly above the sensitivity for TETRA, GSM-R and LTE-R systems, so the interference from the catenary is significant.

REFERENCES

[1] L. Correia, *Mobile Communication Systems*, Slides, Instituto Superior Técnico, Lisbon, Portugal, 2018.

[2] S. H. Masood, *Performance comparison of IEEE 802.11g and IEEE 02.11n in the presence of interference from 802.15.4 networks*, Department of Electrical Engineering, McGill University, Montreal, Quebec, Canada, Aug. 2013. [Online] Available in: (https://arxiv.org/ftp/arxiv/papers/1308/1308.0678.pdf) [Accessed in Oct. 2018].

[3] *Terrestrial Trunked Radio (TETRA) Release 2*, Technical Report, European Telecommunications Standards Institute, Sophia, France, October 2007. [Online] Available in: (https://www.etsi.org/deliver/etsi_tr/102500_102599/102580/01.01.01_60/tr_102580v010101p.pdf)

[4] 3GPP, *Evolved Universal Terrestrial Radio Access (E-UTRA); User Equipment (UE) radio transmission and reception*, Report ETSI TS 36.101, V14.3.0, Release 14, Apr. 2017. [Online] Available in:(http://www.etsi.org/deliver/etsi_ts/136100_136199/136101/14.03.00_60/ts_136101v140300p.pdf) [Accessed in Sep. 2018].

[5] H. Fridhi, V. Deniau, J.P. Ghys, M. Heddebaut, J. Rodriguez and I. Adin, *Analysis of the coupling path between transient EM interferences produced by the catenary-pantograph contact and on-board railway communication antennas*, Univ. Lille Nord de France, IFSTTAR, Villeneuve d'Ascq, France, CAF, Beasain (Guipuzcoa), Spain, CEIT and University of Navarra, Donostia - San Sebastián, Spain, Sep. 2013. [Online] Available in: (https://ieeexplore.ieee.org/document/6632310) [Accessed in Sep. 2018].

[6] B. Tellini; M. Macucci; R. Giannetti; G.A. Antonacci, *Line-pantograph EMI in railway systems*, Pisa University, Italy, Dec. 2001. [Online] Available in: (https://ieeexplore.ieee.org/document/975459) [Accessed in Oct. 2018].

[7] B. Tellini; M. Macucci; R. Giannetti; G.A. Antonacci, *Conducted and Radiated Interference Measurements in the Line-Pantograph System*, IEEE TRANSACTIONS ON INSTRUMENTATION AND MEASUREMENT, Volume 50, Nº 6, Dec. 2001. [Online] Available in: (https://ieeexplore.ieee.org/document/982964/figures#figures) [Accessed in Oct. 2018].

[8] v. Deniau, H. Fridhi, Heddebaut, J. Rioult, I. Adin. and J. Rodriguez, *Analysis and modelling of the EM interference produced above a train associated to the contact between the catenary and the pantograph*, Belgium, Sep. 2013. [Online] Available in: (https://hal.archives-ouvertes.fr/hal-00911695/document) [Accessed in Sep. 2018].

[9] R. Giannetti, M. Macucci, B. Tellini B. Tellini, *Remarks on models for prediction of radiated fields in electrical discharge events*, Electronics Letters, Volume 37, Issue 13, Jun. 2001. [Online] Available in: (https://ieeexplore.ieee.org/abstract/document/933396) [Accessed in Dec 2018].

[10] Surajit Midya, Dierk Bormann, Ziya Mazloom, Thorsten Schutte, Tajeev Thottappillil, *Conducted and radiated emission from pantograph arcing in AC traction syste*m, 2009 IEEE Power & Energy Society General Meeting, Sweden, Jul 2009. [Online] Available in: (https://ieeexplore.ieee.org/document/5275833/authors) [Accessed in Oct. 2018].

[11] M.Mandic, I. Uglesic, V. Milardic, *Study of Electromagnetic Fields from AC 25Kv/50Hz Contact Line Systems*, International Review of Electrical Engineering (I.R.E.E.), vol. xx, nº x, 2007. [Online] Available in: (https://www.researchgate.net/publication/290261770_A_study_of_electromagnetic_fields_from_AC_25_kV50_Hz_contact_line_systems) [Accessed in Oct. 2018].

[12] André Gonçalves Ribeiro, *Analysis of Antennas' Locations on Trains for Mobile Communications*, MSc. Thesis, Instituto Superior Técnico, Universidade de Lisboa, Lisboa, Portugal, Jul. 2018.

[13] Stephen Dudower, Virginie Deniau, M. Nedim Ben Slimen, Ricardo Adriano, *Infrastructures Design, Signalling and Security in Railway, Susceptibility of the GSM-R Transmissions to the Railway Electromagnetic Environment*, 2012. [Online] Available in: (https://www.researchgate.net/publication/224829696_Susceptibility_of_the_GSM-R_Transmissions_to_the_Railway_Electromagnetic_Environment) [Accessed in Sep. 2018].

[14] TL - Train Logistic . [Online] Available in: (https://www.trainlogistic.com/pt/Comboios/Gabinete/fich_atm4000.htm)[Accessed in May 2019].